Rab5 and its effector FHF contribute to neuronal polarity through dynein-dependent retrieval of somatodendritic proteins from the axon

Xiaoli Guo[a,1], Ginny G. Farías[a,1], Rafael Mattera[a], and Juan S. Bonifacino[a,2]

[a]Cell Biology and Neurobiology Branch, Eunice Kennedy Shriver National Institute of Child Health and Human Development, National Institutes of Health, Bethesda, MD 20892

Edited by Pietro De Camilli, Yale University and Howard Hughes Medical Institute, New Haven, CT, and approved July 19, 2016 (received for review February 2, 2016)

An open question in cell biology is how the general intracellular transport machinery is adapted to perform specialized functions in polarized cells such as neurons. Here we illustrate this adaptation by elucidating a role for the ubiquitous small GTPase Ras-related protein in brain 5 (Rab5) in neuronal polarity. We show that inactivation or depletion of Rab5 in rat hippocampal neurons abrogates the somatodendritic polarity of the transferrin receptor and several glutamate receptor types, resulting in their appearance in the axon. This loss of polarity is not caused primarily by increased transport from the soma to the axon but rather by decreased retrieval from the axon to the soma. Retrieval is also dependent on the Rab5 effector Fused Toes (FTS)–Hook–FTS and Hook-interacting protein (FHIP) (FHF) complex, which interacts with the minus-end–directed microtubule motor dynein and its activator dynactin to drive a population of axonal retrograde carriers containing somatodendritic proteins toward the soma. These findings emphasize the importance of both biosynthetic sorting and axonal retrieval for the polarized distribution of somatodendritic receptors at steady state.

Rab5 | FHF complex | dynein | neuronal polarity | retrograde transport

Neurons are highly polarized cells with distinct somatodendritic and axonal domains. Synaptic inputs are received through the somatodendritic domain, integrated at the axon initial segment (AIS), and propagated along the axon for transmission to downstream cells. To accomplish these specialized functions, each neuronal domain is endowed with a distinct set of proteins. A fundamental but still largely unanswered question is how neurons establish and maintain this polarized distribution of proteins throughout their lifetimes. The available evidence indicates that the mechanisms of polarized sorting in neurons are quite complex (1–3). Newly synthesized transmembrane proteins travel together from their site of synthesis in the rough endoplasmic reticulum (ER) to the Golgi complex. Once they reach the *trans*-Golgi network (TGN), the proteins are sorted into different membrane-enclosed transport carriers destined for the somatodendritic or axonal domains (4–8). However, the efficiency of this biosynthetic sorting varies for different proteins and is often incomplete. Other processes, such as compartment-specific retention, retrieval, or transcytosis, additionally contribute to establishing the overall distribution of proteins between the somatodendritic and axonal domains and to their localization to specialized subdomains (5, 9–17).

The selective incorporation of transmembrane proteins into specialized transport carriers is a key event in the mechanisms of polarized sorting. In some cases this process is mediated by recognition of sorting signals in the cytosolic tails of the proteins by components of protein coats associated with the cytosolic face of the donor compartment. One of the best-documented examples is the sorting of various transmembrane proteins to the somatodendritic domain, which depends on interaction of tyrosine-based, dileucine-based, or noncanonical signals in the cytosolic domains of the proteins with the clathrin-associated adaptor protein 1 (AP-1) complex (6, 13, 18–20) or the non–clathrin-associated AP-4 complex (21, 22). After the proteins are packaged into distinct transport carriers, the carriers themselves must be delivered to their corresponding neuronal domains, a process that is driven largely by interaction with specific microtubule motors (23, 24). Axonal microtubules have a uniform orientation with their plus ends pointing toward the distal axon (25). Accordingly, plus-end–directed microtubule motors such as kinesin-1 (e.g., KIF5B) (14, 26) and kinesin-3 (e.g., KIF1A and KIF1Bβ) (27, 28) drive anterograde transport of carrier vesicles and other organelles from the soma to the axon. The opposite process, retrograde transport from the distal axon toward the soma, is mediated by the coupling of carrier vesicles and other organelles to a different type of microtubule motor: the minus-end–directed dynein in complex with dynein activators such as dynactin (29–31). Unlike axons, dendrites of mature hippocampal neurons have microtubule arrays of mixed polarity (32). Consistent with this property, plus-end–directed kinesins (e.g., KIF17) (33), minus-end–directed kinesins (e.g., KIFC2) (34), and the minus-end–directed dynein (35) have all been shown to drive transport of carrier vesicles and organelles into dendrites. Interference with either aspect of sorting—cargo packaging into distinct transport carriers or microtubule-guided delivery of the carriers to their corresponding neuronal domains—alters the polarity of a wide variety of proteins, resulting in their nonpolarized distribution between axon and dendrites.

Significance

Ras-related proteins in brain (Rab) GTPases are general regulators of intracellular traffic in eukaryotic cells, but their specialized roles in neurons are poorly understood. Here we report that Rab5 contributes to the somatodendritic polarity of various surface receptors by mediating their retrieval from the axon. This retrieval is dependent on the Rab5 effector Fused Toes (FTS)–Hook–FTS and Hook-interacting protein (FHIP) (FHF), which in turn interacts with the minus-end–directed microtubule motor dynein–dynactin to drive retrograde transport of receptor-containing carriers from the axon to the soma. These findings reveal a mechanism for coupling axonal retrograde carriers to dynein–dynactin and demonstrate that the somatodendritic polarity of various receptors results from a combination of biosynthetic sorting, the barrier function of the axon initial segment, and retrieval from the axon.

Author contributions: X.G., G.G.F., R.M., and J.S.B. designed research; X.G., G.G.F., and R.M. performed research; X.G., G.G.F., and R.M. analyzed data; and X.G., G.G.F., R.M., and J.S.B. wrote the paper.

The authors declare no conflict of interest.

This article is a PNAS Direct Submission.

[1]X.G. and G.G.F. contributed equally to this work.

[2]To whom correspondence should be addressed. Email: bonifacinoj@helix.nih.gov.

This article contains supporting information online at www.pnas.org/lookup/suppl/doi:10.1073/pnas.1601844113/-/DCSupplemental.

In addition to protein coats and microtubule motors, small GTPases of the Ras-related protein in brain (Rab) family are ubiquitous regulators of protein trafficking and polarized sorting in nonneuronal cells (36). Among the more than 60 Rabs encoded in mammalian genomes, several are known to regulate protein coats (37) or microtubule motors (38). However, the role of Rab proteins in somatodendritic–axonal polarity has not been assessed directly. Here we report that inactivation or depletion of the endosome-associated Rab5 abrogates the somatodendritic polarity of the transferrin receptor (TfR) and several types of glutamate receptor in rat hippocampal neurons. For the TfR, this effect does not result from increased transport from the soma to the axon but from decreased retrieval of a population of TfR that escapes into the axon. TfR retrieval also is dependent on components of a recently described Rab5 effector, the Fused Toes (FTS)–Hook–FTS and Hook-interacting protein (FHIP) (FHF) complex (39–41), previously shown to function as an adaptor of endosomes to the dynein–dynactin complex in filamentous fungi (42–45). These findings uncover a mechanism for axonal retrograde transport involving a Rab5–FHF–dynein–dynactin chain of interactors that promotes retrieval of somatodendritic proteins from the axon. More generally, our observations emphasize the notion that somatodendritic polarity results from a combination of biosynthetic sorting in the soma and retrieval along the length of the axon.

Results

Rab5 Regulates the Somatodendritic Distribution of TfR in Hippocampal Neurons. To identify Rab GTPases that regulate somatodendritic sorting, we cotransfected rat hippocampal neurons with plasmids encoding GFP-tagged, dominant-negative mutant forms of several Golgi or endosomal Rabs and the somatodendritic protein mCherry-TfR at 3 days in vitro (DIV3) and examined the distribution of mCherry-TfR at DIV10 (Fig. 1*A*). Axons were identified by staining for the AIS marker ankyrin G (AnkG) (46), and dendrites were identified by staining for the microtubule-associated protein MAP2 (47). The most striking result was the effect of the dominant-negative GFP-Rab5A-S34N (48, 49), which abrogated the somatodendritic polarity of mCherry-TfR, as evidenced by its appearance in the axon (Fig. 1*A*). Quantification of these results in many neurons showed that the dendrite/axon polarity index of mCherry-TfR decreased from 9.1 ± 1.1 in control neurons expressing GFP to 1.2 ± 0.1 in neurons expressing GFP-Rab5A-S34N (Fig. 1*B*). Under these experimental conditions, expression of GFP-Rab5A-S34N did not alter the overall axonal–somatodendritic organization of most neurons, as evidenced by the normal appearance of the AIS and the somatodendritic polarity of MAP2 (Fig. 1*C*). However, the dendrites appeared shorter and less branched in GFP-Rab5A-S34N–expressing neurons, in line with previous

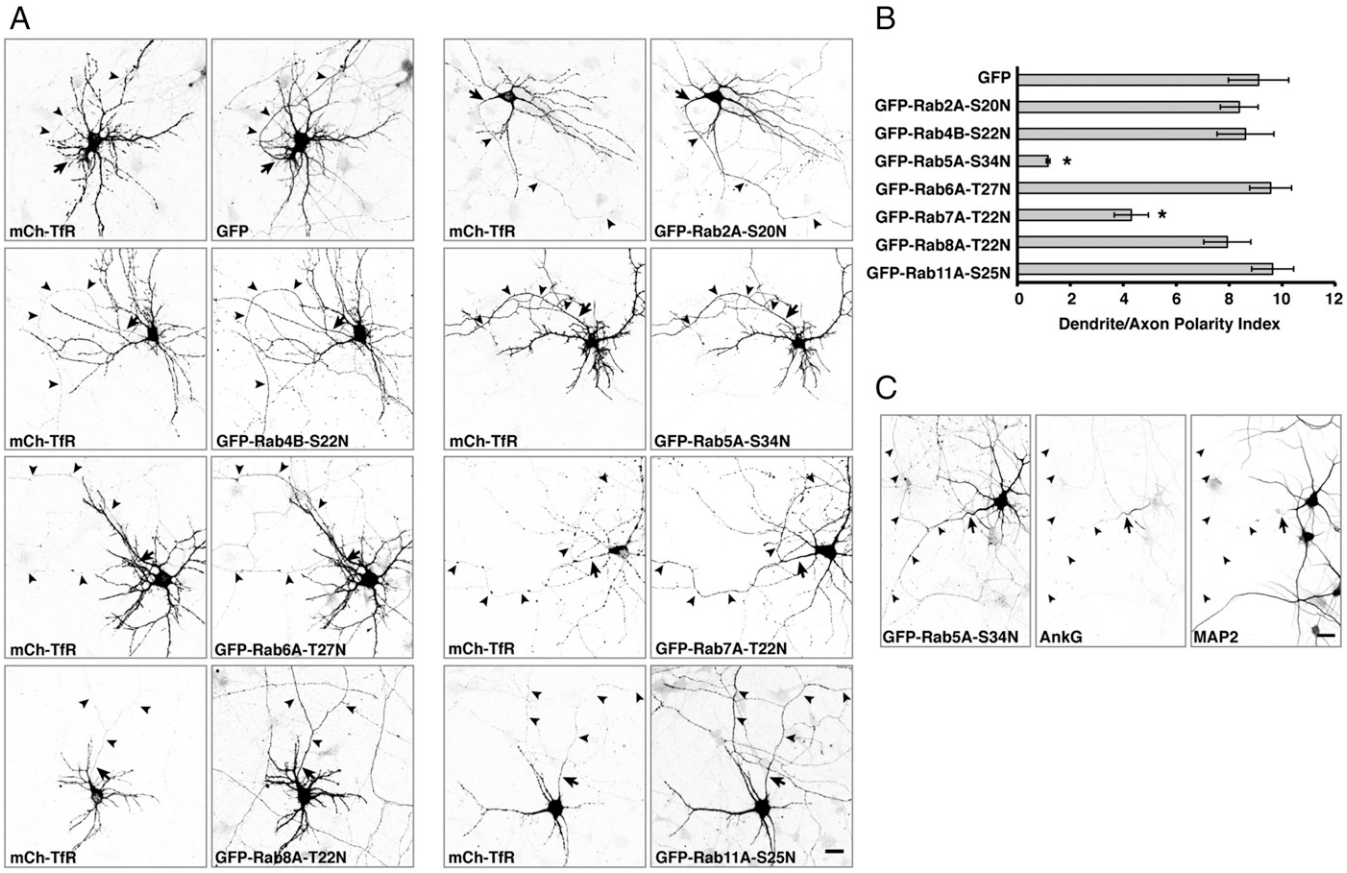

Fig. 1. Effect of dominant-negative Rabs on the somatodendritic polarity of the TfR. (*A*) Rat hippocampal neurons were cotransfected at DIV3 with plasmids encoding mCherry (mCh)-TfR together with GFP (control) or dominant-negative GFP-Rab2A-S20N, GFP-Rab4B-S22N, GFP-Rab5A-S34N, GFP-Rab6A-T27N, GFP-Rab7A-T22N, GFP-Rab8A-T22N, or GFP-Rab11A-S25N. At DIV10, the neurons were fixed, immunostained for AnkG (an AIS marker), and imaged by confocal microscopy. In these and all subsequent experiments, analysis of receptor polarity was performed only on neurons that exhibited a normal appearance of the AIS. (*B*) Dendrite/axon polarity indexes for TfR are represented as the mean ± SEM from 8–20 neurons in at least three independent experiments such as that described in *A*. $^*P < 0.01$ per one-way ANOVA followed by Dunnett's test, compared with GFP control. (*C*) Neurons cotransfected at DIV3 with mCherry-TfR and GFP-Rab5A-S34N were immunostained at DIV10 for AnkG and MAP2 (a somatodendritic marker). In both *A* and *C*, images are shown in negative grayscale. Arrows mark the position of the AIS, and arrowheads indicate the axon. (Scale bars: 20 μm.) In *A*, notice the presence of mCherry-TfR in the axon of GFP-Rab5A-S34N–expressing neurons.

studies demonstrating a role for Rab5 in dendrite morphogenesis (50, 51). A similar loss of TfR-GFP polarity was observed upon cotransfection with mCherry-Rab5A-S34N at DIV5 and analysis of TfR-GFP distribution at DIV7 (Fig. S1). Expression of a GFP-tagged, dominant-negative mutant of the late-endosomal Rab7A also decreased the somatodendritic polarity of mCherry-TfR (polarity index 4.3 ± 0.6), albeit to a lesser extent than expression of GFP-Rab5A-S34N (Fig. 1 *A* and *B*). In contrast, the analogous GFP-tagged, dominant-negative mutants of Rab2A, Rab4B, Rab6A, Rab8A, and Rab11A had no effect on the somatodendritic polarity of mCherry-TfR (Fig. 1 *A* and *B*). The specific requirement of Rab5 activity for TfR polarity was unexpected, because this receptor was not known to traffic through early endosomes en route to the somatodendritic domain. This finding prompted us to study in more detail the role of Rab5 in somatodendritic sorting.

Rab5 Is Required for Somatodendritic Sorting of Glutamate Receptors. To determine if Rab5 regulates the somatodendritic sorting of other cargos, we examined the effect of expressing mCherry-tubulin (control) or mCherry-Rab5A-S34N on the distribution of the ionotropic AMPA-type GluR1 and GluR2, the ionotropic NMDA-type NR2A and NR2B, and the metabotropic mGluR1 glutamate-receptor proteins tagged with GFP or superecliptic pHluorin (SEP) (Fig. 2 *A* and *B*). We observed that all these receptor proteins were most concentrated in the somatodendritic domain in control cells (Fig. 2 *A* and *C*) but became nonpolarized in Rab5A-S34N–expressing cells (Fig. 2 *B* and *C*). To confirm the requirement of Rab5 for the polarized sorting of these receptors, we additionally used shRNAs to abrogate the expression of all three isoforms of Rab5 (A, B, and C) (52) (hereafter referred to as "Rab5-shRNA"). Immunofluorescence microscopy showed that endogenous Rab5 was largely depleted in Rab5-shRNA–transfected neurons (Fig. S2 *A* and *B*). In agreement with the

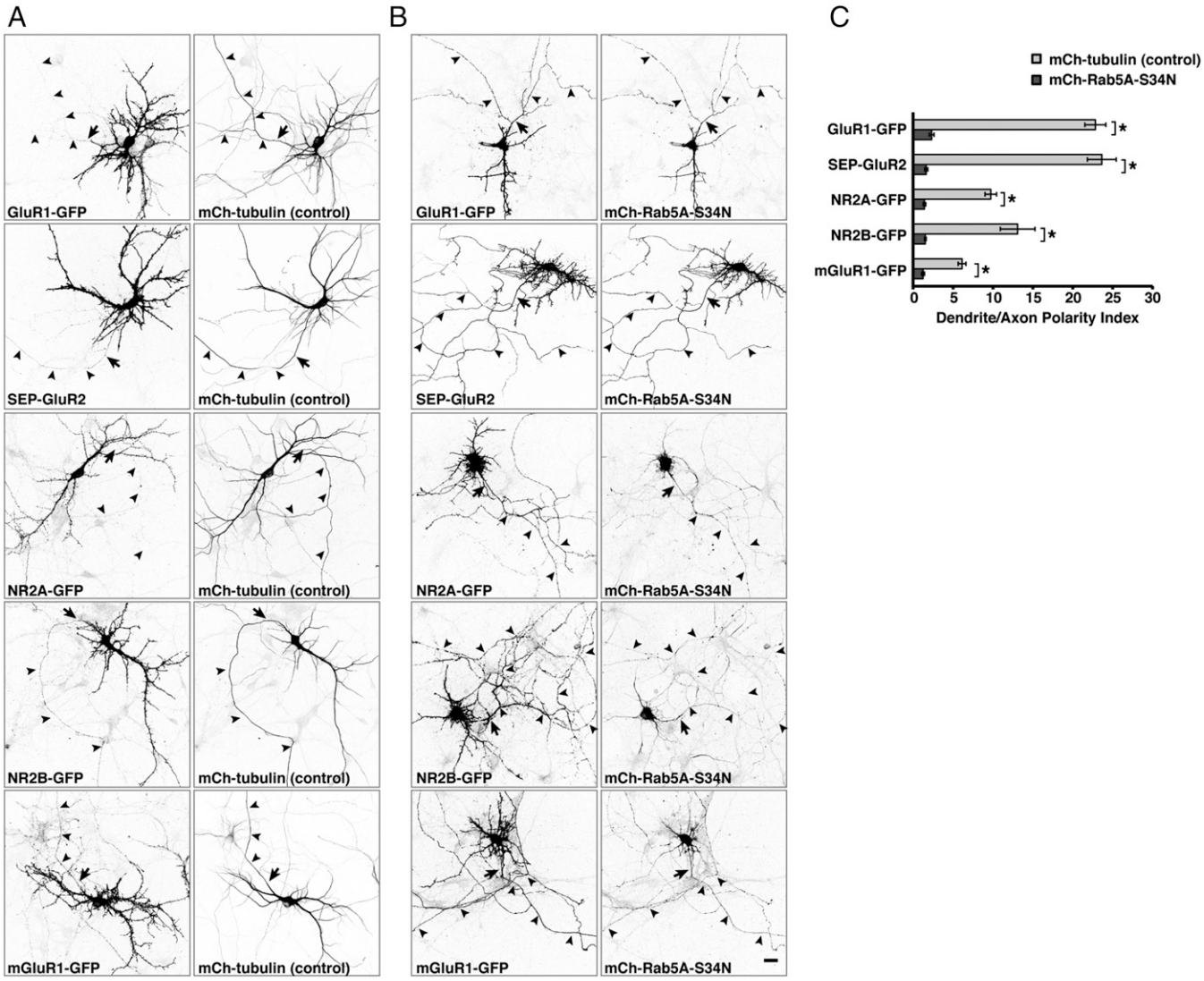

Fig. 2. Expression of dominant-negative Rab5A abolishes the somatodendritic polarity of glutamate receptors. (*A* and *B*) Rat hippocampal neurons were cotransfected at DIV4 with plasmids encoding GluR1-GFP, SEP-GluR2, NR2A-GFP, NR2B-GFP, or mGluR1-GFP together with plasmids encoding mCherry (mCh)-tubulin (control) (*A*) or dominant-negative mCherry-Rab5A-S34N (*B*). Fixed neurons were immunostained at DIV9 for GFP and AnkG and were imaged by confocal microscopy. Images are shown in negative grayscale. Arrows mark the position of the AIS, and arrowheads indicate the axon. (Scale bar: 20 μm.) (*C*) Dendrite/axon polarity indexes for glutamate receptors are represented as the mean ± SEM from 10 neurons in at least three independent experiments such as those shown in *A* and *B*. $*P < 0.01$ per Student's *t* test. Notice that expression of mCherry-Rab5A-S34N abrogates the somatodendritic polarity of all the glutamate receptor proteins.

results of dominant-negative Rab5A expression, we found that all the transgenic glutamate receptors localized to the somatodendritic domain in neurons transfected with mCherry control plasmid (Fig. S2 *E* and *G*) but appeared in the axon in neurons transfected with the Rab5-shRNA plasmids (Fig. S2 *F* and *G*). A similar loss of polarity was observed for endogenous TfR, GluR1, GluR2, and NR2A in neurons transfected with Rab5-shRNA plasmid (Fig. 3 *A* and *B*). Taken together, these results revealed that the somatodendritic polarity of at least six different proteins (i.e., the TfR and five glutamate receptor proteins) depends on Rab5, demonstrating a general role of this Rab in somatodendritic sorting.

Rab5 Promotes Axonal Retrograde Transport of the TfR. We next addressed how interference with Rab5 increased the levels of TfR in the axon. Rab5 was previously shown to associate with both somatodendritic and axonal endosomes in rat hippocampal neurons (53–55). Consistent with the somatodendritic polarity of the TfR, most mCherry-TfR was found in somatodendritic foci, many of which exhibited colocalization with GFP-Rab5A (Fig. 4*A*). Increasing the gain in the confocal microscope revealed smaller amounts of mCherry-TfR in axonal foci, where it also showed colocalization with GFP-Rab5A (Fig. 4*A*). Live-cell imaging and kymograph analysis of mCherry-TfR foci at an axonal segment adjacent to the distal edge of the AIS showed the presence of this protein in faint anterograde carriers (lines with negative slopes in the kymographs) and brighter retrograde carriers (lines with positive slopes) as well as in stationary foci (vertical lines) (Fig. 4*B* and Movie S1). Notably, GFP-Rab5A and mCherry-TfR colocalized predominantly on the retrograde carriers and stationary foci (Fig. 4 *B* and *C*). Retrograde carriers containing TfR-GFP were observed throughout the axon, including the AIS (Figs. S3 and S4), but were relatively less abundant at the axon terminal, where most TfR-GFP foci were stationary (Fig. S3).

Loss of somatodendritic polarity of the TfR upon interference with Rab5 could result from either increased anterograde transport or decreased retrograde transport of TfR in the axon. To distinguish between these possibilities, we transfected neurons with plasmids encoding TfR-GFP and either mCherry-tubulin (control) or Rab5-shRNA (also expressing mCherry). We photobleached a segment of the proximal axon located 25–35 μm beyond the distal edge of the AIS (boxed area in Fig. 4*D*) and monitored by live-cell imaging and kymograph analysis the anterograde and retrograde TfR-GFP carriers entering the photobleach box over a 450-s period (Fig. 4 *D* and *E* and Movie S2). This analysis showed a much smaller flux of TfR carriers into the photobleach box in Rab5-depleted neurons relative to control neurons (Fig. 4 *D* and *E* and Movie S2). Most importantly, although no increase in the number of anterograde TfR carriers was visible, there was a dramatic decrease in the number of retrograde TfR carriers entering the photobleach box in the Rab5-depleted neurons (Fig. 4 *D* and *E* and Movie S2). Similar results were obtained when photobleaching was performed on the AIS itself (Fig. S4 and Movie S3). From these experiments, we concluded that Rab5 contributes to the somatodendritic polarity of TfR by promoting the retrieval of a population of TfR that escapes into the axon.

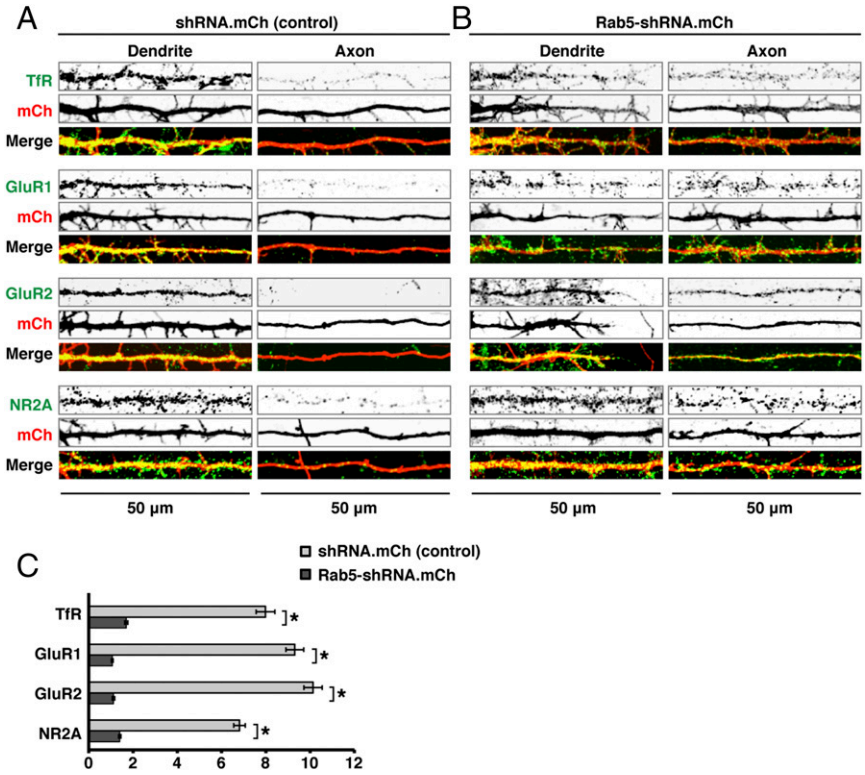

Fig. 3. Expression of Rab5-shRNA abrogates the somatodendritic polarity of various endogenous receptors. (*A* and *B*) Rat hippocampal neurons were transfected at DIV5 with a scrambled shRNA control plasmid (*A*) or Rab5-shRNA–expressing plasmid (*B*), both also driving expression of mCherry. Neurons were fixed and immunostained at DIV10 for the endogenous receptor proteins TfR, GluR1, GluR2, or NR2A, together with AnkG for distinction of dendrites and axons. The distribution of the receptor proteins was imaged by confocal microscopy. Fifty-micrometer segments of dendrites and axons immediately distal to the AIS are shown. (*C*) Dendrite/axon polarity indexes are represented as the mean ± SEM from 10 neurons in three independent experiments such as described in *A* and *B*. $^*P < 0.01$ per Student's *t* test. Note that transfection with Rab5-shRNA plasmid abrogates the somatodendritic polarity of endogenous TfR, GluR1, GluR2, and NR2A.

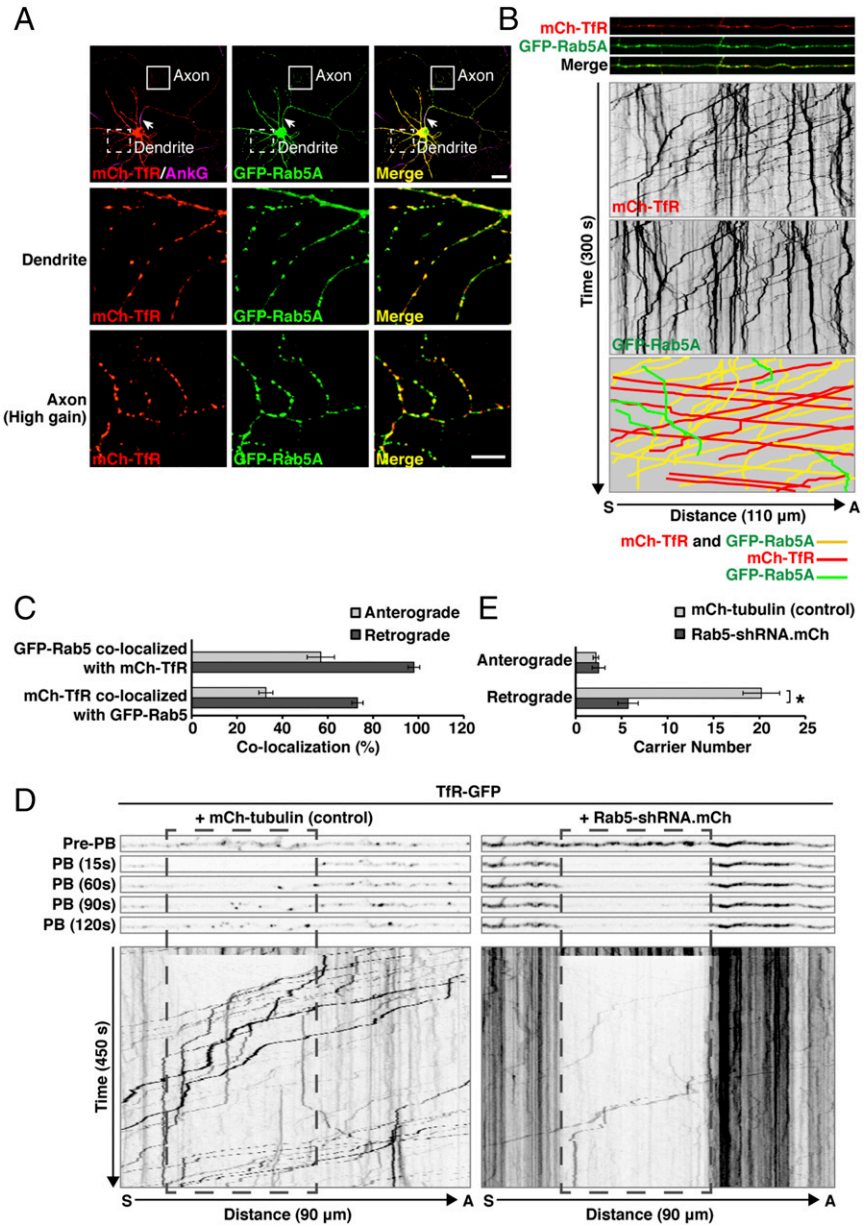

Fig. 4. Rab5 depletion reduces axonal retrograde transport of the TfR. (*A*) Colocalization of Rab5 with TfR. Rat hippocampal neurons cotransfected at DIV3 with plasmids encoding mCherry (mCh)-TfR and GFP-Rab5A were immunostained at DIV10 for AnkG. Fixed neurons were imaged by confocal microscopy. Arrows indicate the position of the AIS. Magnifications of the boxed regions in the top row are shown in the middle and bottom rows. In the bottom row, brightness (i.e., gain) was increased to enhance the weak mCherry-TfR fluorescence in the axon. (Scale bars: 20 μm for the top row; 10 μm for the middle and bottom rows.) (*B*) Rat hippocampal neurons transfected as in *A* were surface-labeled at DIV8 with CF640-conjugated antibody to the AIS marker neurofascin and analyzed by live-cell imaging. Dual-color images of an axon segment adjacent to the distal edge of the AIS were acquired sequentially at 1-s intervals. The three top strips show single frames, and the two middle panels show negative grayscale kymographs from Movie S1. The bottom panel represents the trajectories of carriers having both GFP-Rab5A and mCherry-TfR (yellow lines), only GFP-Rab5A (green), or only mCherry-TfR (red). Lines with negative and positive slopes represent carriers moving in anterograde and retrograde directions, respectively. Vertical lines represent stationary foci. (*C*) Quantification of colocalization of GFP-Rab5A and mCherry-TfR in anterograde and retrograde carriers. Values are the mean ± SEM from proximal axon segments of six neurons imaged as in *B*. (*D*) Rat hippocampal neurons were transfected at DIV3 with plasmids encoding TfR-GFP together with mCherry-tubulin (control) or Rab5-shRNA also expressing mCherry and imaged live at DIV8 after surface-labeling with CF640-conjugated antibody to the AIS marker neurofascin. An axonal segment 25–35 μm distal to the AIS was photobleached (PB), and TfR-GFP–containing carriers entering the photobleach box were imaged at 1.5-s intervals. The five upper strips, extracted from Movie S2, show frames before photobleaching (pre-PB) and after 15, 60, 90, and 120 s of fluorescence recovery. The lower panels, also from Movie S2, show negative grayscale kymographs after up to 450 s of fluorescence recovery. (*E*) Quantification of the number of TfR-GFP–containing anterograde and retrograde carriers entering the photobleach box. Values are the mean ± SEM from 9–12 axons imaged as in *D*. $*P < 0.01$ per Student's *t* test.

Additional fluorescence microscopy experiments showed that most axonal TfR-GFP foci in neurons expressing mCherry-Rab5A-S34N or Rab5-shRNA accumulated internalized Alexa 647-conjugated transferrin (Tf-Alexa 647) (Fig. S5), indicating that this TfR population was capable of mediating endocytosis despite inactivation or depletion of Rab5. In addition, live-cell imaging of control neurons revealed that internalized Tf-Alexa 647 was present mainly in stationary foci and retrograde carriers

(Fig. S6 and Movie S4), demonstrating that both these structures have characteristics of endosomes.

TfR Retrieval from the Axon Is Dependent on Dynein–Dynactin. How could Rab5 regulate TfR retrieval from the axon? It is well known that axonal retrograde transport of various organelles is driven by dynein in complex with its activator dynactin (29–31). Indeed, previous studies showed that disruption of dynein function caused mislocalization of somatodendritic organelles and proteins to the axon [e.g., Golgi outposts and the ion channel Pickpocket in *Drosophila* neurons (56); GluR2 in rat hippocampal neurons (57)], although these effects were largely attributed to a role of dynein in transport to the dendrites. Using live-cell imaging, we observed that GFP-labeled dynein intermediate chain IC2C (58) (indicated as GFP-Dynein) was mostly cytosolic when expressed alone. However, when GFP-IC2C was coexpressed with mCherry-Rab5A, both proteins were found in association with a population of axonal retrograde carriers (Fig. 5*A* and Movie S5). In addition, we observed that overexpression of either the mCherry-labeled p50 (dynamitin) subunit of the dynein regulator dynactin (59) or the mCherry-labeled CC1 domain of the $p150^{Glued}$ subunit of dynactin (60), both known to cause disassembly of the dynein–dynactin complex, increased the levels of TfR-GFP in the axon (Fig. 5 *B* and *C*). These findings raised the possibility that Rab5 exerts its role in retrograde transport and somatodendritic polarity of the TfR primarily through regulation of the dynein–dynactin complex.

The Mammalian FHF Complex Is a Rab5 Effector. Rab5 interacts with more than 25 different effector proteins to promote the motility (61), fusion (62), and signaling properties (63) of early endosomes. To date, however, none of these effectors has been shown to link Rab5 to dynein–dynactin. A recent screen for Rab interactors in *Drosophila* identified the orthologs of subunits of the mammalian FHF complex in affinity purifications using the GTP-locked form of *Drosophila* Rab5 as bait (41). The mammalian FHF complex comprises three subunits, FTS, Hook, and FHIP (40); Hook occurs as three isoforms (Hook1, Hook2, and Hook3) encoded by different genes (40, 64). Importantly, in filamentous fungi the FHF complex couples early endosomes to dynein–dynactin, promoting their movement toward microtubule minus ends (42, 44, 65). The mammalian Hook3 protein also was found to interact with dynein–dynactin, promoting its highly processive movement along microtubules in vitro (43). We thus hypothesized that the role of Rab5 in promoting axonal retrograde transport and somatodendritic polarity of the TfR could be mediated by the mammalian FHF complex. To test this hypothesis, we first performed pull-down assays using GST fused to mammalian Rab5A-WT, GTP-locked Rab5A-Q79L, or GDP-locked Rab5A-S34N (Fig. 6*A*) and a detergent extract from human HEK293T cells. We observed robust and specific pulldown of Hook1, Hook3, and FHIP by Rab5A-Q79L but not by Rab5A-WT or Rab5A-S34N (Fig. 6*B*). The behavior of Hook2 was qualitatively similar, although the pulldown was much weaker (Fig. 6*B*). In contrast, we could not detect pulldown of FTS under any of the conditions tested (Fig. 6*B*), perhaps because of dissociation from the complex during the procedure or the existence of alternative FHF assemblies. The existence of FHF variants would be consistent with reported differences in the intracellular localization and function of the three Hook subunit isoforms (64, 66, 67). These results demonstrated that a mammalian FHF complex comprised of at least Hook1, Hook3, and FHIP has the biochemical properties of a bona fide Rab5 effector.

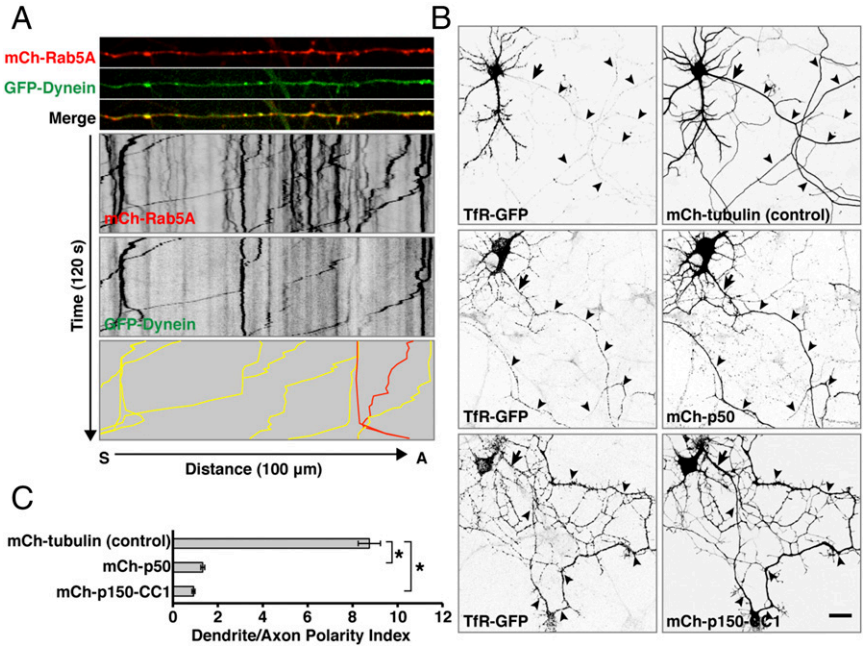

Fig. 5. Somatodendritic polarity of the TfR depends on dynein–dynactin. (*A*) Rat hippocampal neurons were transfected at DIV4 with a plasmid encoding the IC2C dynein intermediate chain fused to GFP (indicated as GFP-Dynein) together with plasmids encoding mCherry (mCh)-Rab5A and were examined at DIV8 by live-cell imaging and kymograph analysis. Dual-color images of midaxon segments were acquired sequentially at 1-s intervals for 120 s. The top three strips show single frames, and the two middle panels show negative grayscale kymographs (all from Movie S5). The bottom panel represents the trajectories of carriers having mCherry-Rab5A together with GFP-Dynein (yellow lines) or only mCherry-Rab5A (red lines). (*B*) Rat hippocampal neurons were cotransfected at DIV4 with plasmids encoding TfR-GFP together with tubulin (control), the p50 subunit of dynactin, or the CC1 domain of the $p150^{Glued}$ subunit of dynactin, all tagged with mCherry. At DIV8, neurons were fixed and immunostained for AnkG and were imaged by confocal microscopy. Images are shown in negative grayscale. Arrows mark the position of the AIS, and arrowheads indicate the axon. (Scale bar: 20 μm.) (*C*) Dendrite/axon polarity indexes for TfR from experiments such as that described in *B* are represented as the mean ± SEM from 20 neurons in at least three independent experiments. $*P < 0.01$ per one-way ANOVA followed by Dunnett's test.

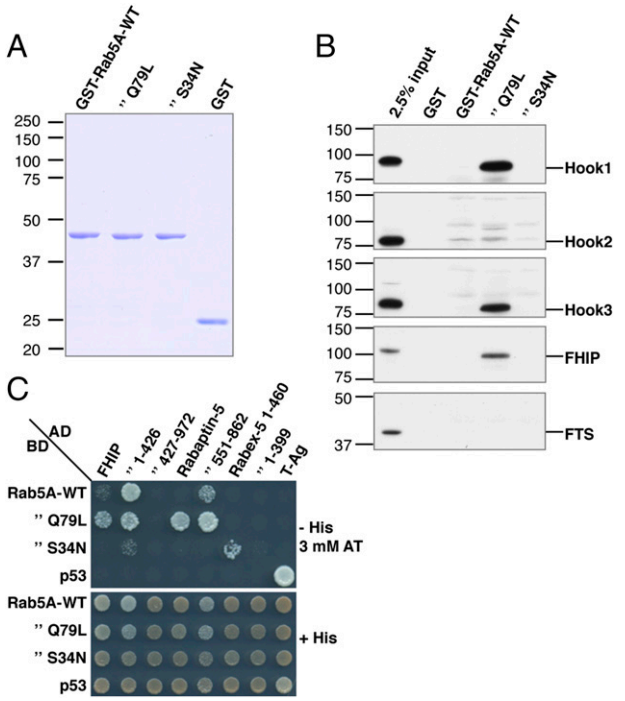

Fig. 6. A complex containing Hook1/3 and FHIP behaves as a Rab5 effector. (*A*) Coomassie blue staining of GST fusion proteins used in the experiment. (*B*) Pulldown of FHF complex subunits from HEK293T cell extracts by GST-Rab5A proteins. Bound proteins were eluted and were analyzed by SDS/PAGE and immunoblotting with antibodies to the proteins indicated at right. The positions of molecular mass markers (in kilodaltons) are indicated at left. The signal in pulled-down complexes relative to input (first lane at left) indicates preferential interaction of GST-Rab5A-Q79L with Hook1, Hook3, and FHIP. (*C*) Yeast two-hybrid assays demonstrate direct, activation-dependent interaction of Rab5A with FHIP. Growth on selective plates without His (−His) is indicative of interactions (*Upper*), and incubation on plates containing His (+His) is a control for growth/loading of double transformants (*Lower*). The −His plates were supplemented with 3 mM 3-amino-1,2,4-triazole (AT), a competitive inhibitor of the His3 protein, to increase the stringency of the assay. The Rabaptin-5 full-length and 551–862 fragments (84) were used as controls for preferential interaction with Rab5A-Q79L. The Rabex-5 constructs 1–460 and 1–399 (69) served as controls for preferential interaction with Rab5A-S34N (longer incubation times were required to detect interaction with Rabex-5 1–399). Double transformations of Gal4-binding domain (BD) constructs with SV40 large T-antigen (T-Ag) and of Gal4 activation domain (AD) constructs with p53 provided negative controls. Double transformation with T-Ag and p53 plasmids served as an additional positive control.

In filamentous fungi, FHIP is capable of associating with endosomes independently of Hook and FTS (65). To determine whether such an association in mammalian cells could be mediated by interaction with Rab5, we tested for interaction of FHIP with Rab5A-WT, Rab5A-Q79L, and Rab5A-S34N using the yeast two-hybrid system (Fig. 6*C*). Indeed, we observed that FHIP interacted with Rab5A-Q79L more strongly than with Rab5A-WT or Rab5A-S34N (Fig. 6*C*), as expected for a true Rab5 effector. The N-terminal half of FHIP (residues 1–426) interacted even more robustly with Rab5A-Q79L and also exhibited strong interaction with Rab5A-WT (Fig. 6*C*). This behavior was similar to that of the previously characterized Rab5 effector Rabaptin-5 (Fig. 6*C*) (68). In contrast, the control protein Rabex-5 interacted with Rab5A-S34N but not with Rab5A-WT or Rab5A-Q79L (Fig. 6*C*), as expected from its role as a Rab5 guanine nucleotide-exchange factor (GEF) (69, 70). We concluded that FHIP interacts directly and in a nucleotide-dependent manner with Rab5A, as is consistent with its being the subunit that recruits the FHF complex to endosomes (65).

Hoook1/3 and FHIP Are Required for Somatodendritic Sorting of the TfR. Hook1 and Hook3, the two isoforms pulled down by Rab5A, are expressed predominantly in neurons, whereas Hook2 is expressed mainly in astrocytes (71). Imaging of live neurons and kymograph analysis showed that mCherry-labeled forms of both Hook1 and Hook3, as well as FHIP-mCherry, colocalized with GFP-Rab5A on axonal retrograde carriers (Fig. 7*A* and Movie S6). In addition, we observed that shRNA-mediated knockdown of Hook1, Hook3, or FHIP resulted in increased levels of mCherry-TfR in the axon, with consequent loss of its somatodendritic polarity (Fig. 7 *B* and *C*). Taken together, the results of our experiments are consistent with a role of Hook1/3 and FHIP in linking Rab5-containing carriers to dynein–dynactin, thus promoting axonal retrograde transport of TfR-containing carriers and contributing to the somatodendritic polarity of the TfR at steady state (Fig. 8).

Discussion

The results presented here demonstrate that the endosome-associated Rab5 contributes to neuronal polarity by mediating the retrieval of a population of missorted somatodendritic receptors from the axon to the soma. Inactivation or depletion of Rab5 causes a dramatic loss of somatodendritic polarity in several receptors, including the TfR and various glutamate receptors. We initially entertained the hypothesis that this loss of polarity was caused by failure of polarized sorting in an endosomal compartment in the neuronal soma. This possibility would be in line with previous studies supporting a transendosomal route for the biosynthetic delivery of TfR to the plasma membrane in nonneuronal cells (72, 73). However, our photobleaching and live-cell imaging experiments showed that depletion of Rab5 did not result in increased transport of TfR from the soma to the axon but rather in its decreased retrieval from the axon to the soma (Fig. 4). These findings emphasize the notion that the polarized distribution of proteins between the axonal and somatodendritic domains at steady state results from a combination of biosynthetic sorting in the soma, the barrier function of the AIS, and retrieval from the axon.

Retrieval of somatodendritic proteins appears to occur at several stages on the way from the TGN to the distal axon. The majority of somatodendritic carriers budding from the TGN are prevented from entering the axon at a preaxonal exclusion zone (PAEZ) in the cytoplasm of the axon hillock (8). Of the remaining carriers that manage to penetrate this zone, some reverse direction at the PAEZ (8) or the AIS (7, 8, 14, 15, 17, 74), in the latter segment through acquisition of myosin Va (15) and/or dynein (17) motors. Our findings now show that still another population of somatodendritic proteins that escapes sorting at the TGN, PAEZ, and/or AIS can be retrieved from more distal parts of the axon by a Rab5-dependent mechanism. This mechanism does not appear to involve a simple reversal in the direction of somatodendritic carriers, because the axonal retrograde carriers differ in being brighter and having early endosomal contents such as internalized transferrin (Tf). Most likely, the escaped somatodendritic proteins are delivered to the plasma membrane and/or endosomes along the axon before their packaging into retrograde carriers. Interference with any of these sequential mechanisms leads to progressive buildup of somatodendritic proteins in the axon, highlighting the importance of iterative axonal retrieval for the maintenance of neuronal polarity.

Over the past decade, several studies have implicated Rab5 in axonal retrograde transport of tetanus neurotoxin (55), the neurotrophins nerve growth factor and brain-derived neurotrophic factor and their receptors $p75^{NTR}$ and Trk (75, 76), and the adenovirus CAV-2 and its receptor coxsackievirus and adenovirus receptor (CAR) (77), in motor neurons and dorsal root ganglia neurons. In most of these cases, Rab5 was shown to act at an early step in the distal axon by promoting endocytosis followed by transfer of the internalized ligands and their receptors

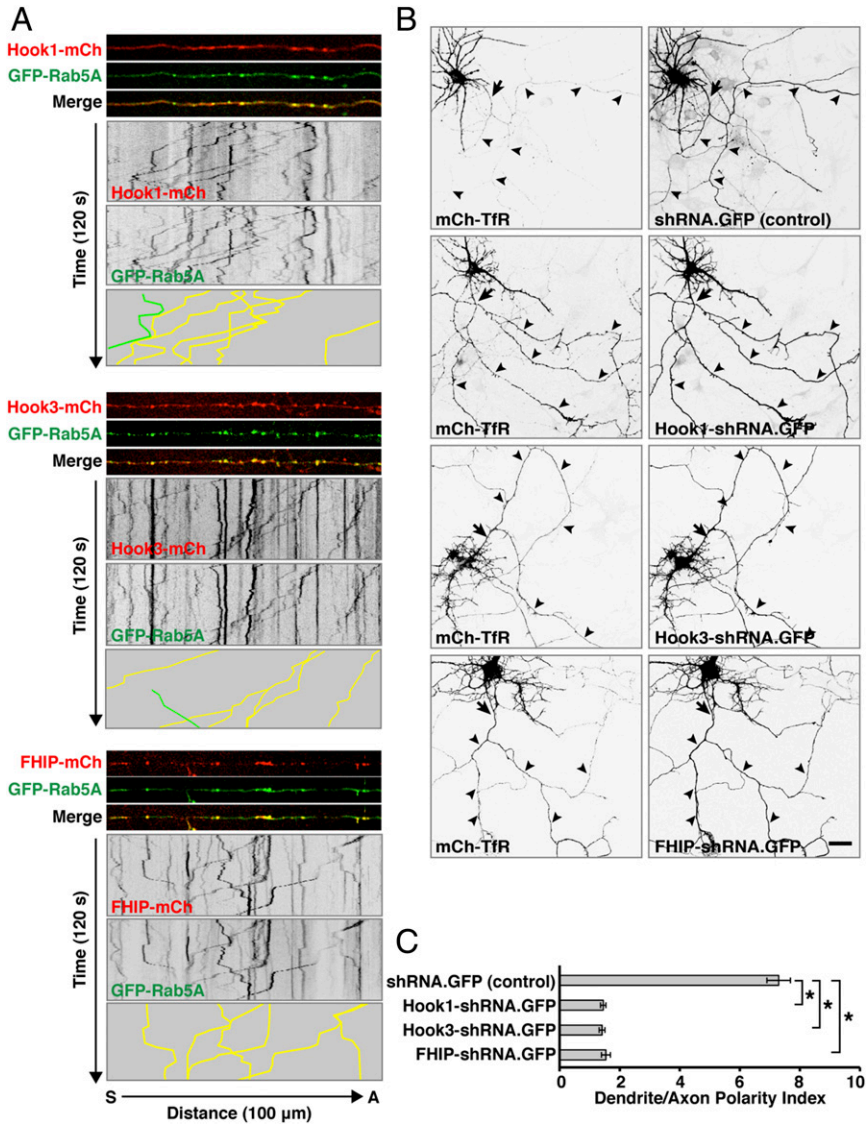

Fig. 7. Somatodendritic polarity of the TfR depends on components of the FHF complex. (*A*) Rat hippocampal neurons were transfected at DIV4 with plasmids encoding GFP-Rab5A together with Hook1, Hook3, or FHIP, all tagged with mCherry, and were examined by live-cell imaging and kymograph analysis at DIV8. Dual-color images of midaxon segments were acquired sequentially at 1-s intervals for 120 s (Movie S6). For each FHF component, the three top strips show single frames, the two middle panels show negative grayscale kymographs, and the bottom panel represents the trajectories of carriers having both GFP-Rab5A and an mCherry-tagged FHF subunit (yellow lines) or only GFP-Rab5A (green lines). (*B*) Rat hippocampal neurons were cotransfected at DIV4 with plasmids encoding mCherry-TfR together with plasmids encoding shRNAs targeting Hook1, Hook3, or FHIP as well as GFP. Fixed neurons were immunostained at DIV8 for AnkG and were imaged by confocal microscopy. In this figure images for mCherry and GFP are shown in negative grayscale. Arrows indicate the position of the AIS, and arrowheads indicate the trajectory of the axon. (Scale bar: 20 μm.) (*C*) Dendrite/axon polarity indexes for TfR from experiments such as those described in *B* are represented as the mean ± SEM from 20 neurons in at least three independent experiments. $^*P < 0.01$ per one-way ANOVA followed by Dunnett's test.

to Rab7-associated carriers that then undergo retrograde transport toward the soma. Although in previous studies Rab5 was found in foci distributed throughout the axon, most of these foci were reportedly static or oscillatory and did not translocate over long distances. The effects of inactivating or depleting Rab5 on the polarized distribution of TfR observed in our study could be explained in part by inhibition of internalization or transfer to Rab7-associated retrograde carriers in the distal axon. However, TfR-containing foci in Rab5-deficient cells were accessible to internalized Tf (Fig. S5). Moreover, although treatment with an shRNA targeting the μ2 subunit of AP-2 inhibited TfR endocytosis, it did not alter the somatodendritic polarity of the TfR (6). Finally, the expression of dominant-negative Rab7A had less effect on TfR polarity than the expression of dominant-negative Rab5A (an approximately twofold vs. an approximately eightfold decrease, respectively) (Fig. 1). These findings suggested that Rab5 has an additional role in retrograde transport.

In our experiments, we confirmed that many Rab5 foci were static, but we also observed a population of rapidly moving Rab5-containing retrograde carriers along the axon of hippocampal neurons (Figs. 4, 5, and 7). The majority of the static and retrogradely moving Rab5 foci also contained TfR (Fig. 4 *B* and *C*) and internalized Tf (Figs. S5 and S6), suggesting that they were early endosomal in nature and likely were distinct from the Rab7-associated carriers that transport neurotrophins and their receptors. In nonneuronal cells, Rab7 recruits its effectors RILP and ORP1L to late endosomes, linking them to dynein–dynactin for centripetal transport toward microtubule minus ends (78–80).

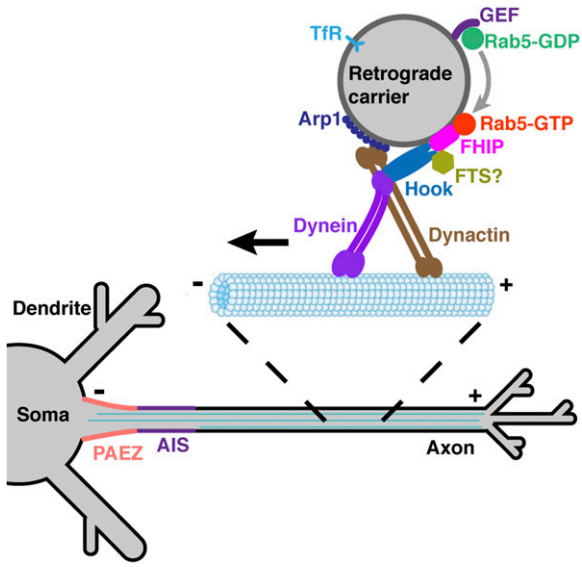

Fig. 8. Schematic representation of the role of Rab5, the FHF complex, and dynein–dynactin in axonal retrieval of the TfR. A population of somatodendritic proteins that escape into the axon is packed into Rab5-associated retrograde carriers. The GTP-bound form of Rab5 recruits its effector FHF complex via an interaction with the FHIP subunit. The Hook subunits of FHF then bind the minus end-directed microtubule motor dynein–dynactin (42–44), promoting retrograde movement of the transport carriers. Rab5 and FHF thus function as a regulated adaptor complex for coupling of TfR-containing retrograde carriers to dynein–dynactin.

A similar mechanism might be responsible for the transport of Rab7-associated carriers in neurons. Nevertheless, the existence of retrograde carriers containing Rab5 and TfR presented the problem that Rab5 was not known to be physically coupled to dynein–dynactin. The recent identification of FHF subunit orthologs as nucleotide-dependent interactors of Rab5 in *Drosophila* (41) and the role of the FHF complex in coupling early endosomes to dynein–dynactin in filamentous fungi (42–44, 65) suggested a possible link. Indeed, we found that the mammalian Hook1/3 and FHIP subunits of FHF preferentially interacted with the GTP-bound form of Rab5 (Fig. 6), that they comoved with Rab5A-containing axonal retrograde carriers (Fig. 7*A* and Movie S6), and that their depletion abrogated TfR somatodendritic polarity (Fig. 7 *B* and *C*). From these results, we concluded that the mammalian FHF complex is a Rab5 effector that may couple TfR-containing axonal retrograde carriers to dynein–dynactin.

It is worth mentioning that interference with Rab5 (Figs. 1 and 3) or the FHF complex (Fig. 7) did not lead to complete accumulation of TfR at axon tips. This finding might be explained by the retrieval occuring at sites along the entire length of the axon and not just at axon terminals. Additionally, Rab7 and its effectors could promote some retrieval, as discussed above. Moreover, Hook has also been shown to act as an adaptor for the plus-end–directed kinesin-3 motor in filamentous fungi (42). If Hook had a similar function for some of the ∼10 kinesin-3 family members in mammals, then the effect of interfering with Hook proteins potentially could affect axonal anterograde transport of TfR as well. The faintness of the TfR-containing anterograde carriers prevented us from reliably quantifying an effect of Rab5-FHF interference on the motility of these carriers.

On the basis of these observations, we propose the scheme shown in Fig. 8. A Rab5 GEF exchanges GTP for GDP on Rab5, promoting Rab5 recruitment to a population of axonal retrograde carriers containing TfR. This recruitment initiates a chain of interactions involving the FHF complex and dynein–dynactin that drives transport of the carriers toward the soma. This mechanism is alternative to that involving Rab7 and may be particularly relevant for the retrograde transport of carriers with characteristics of early endosomes, including those that retrieve somatodendritic proteins from the axon to the soma. We speculate that axonal transmembrane receptors that deliver signals from early rather than late endosomes also might be transported to the soma within this population of retrograde carriers. Mutations in the Rab5 GEF alsin (81) and in components of the dynein–dynactin complex (82, 83) are causes of neurodegenerative disorders in humans. Failure of the mechanism described here could account in part for the trafficking defects, axonal degeneration, and neuronal death that underlie these disorders.

Materials and Methods

Recombinant constructs, antibodies, culture and transfection of rat hippocampal neurons, fluorescence microscopy and imaging analysis, GST-fusion protein expression and purification, GST-pulldown assays, and yeast two-hybrid assays are described in *SI Materials and Methods*. Animal use was in accordance with all NIH and US government regulations, under Animal Study Proposal (ASP) 13-011 approved by the National Institute of Child Health and Human Development Animal Care and Use Committee.

ACKNOWLEDGMENTS. We thank X. Zhu for expert technical assistance; J. W. Harper, H. Krämer, C. Schindler, and M. Zerial for generous gifts of reagents; and X. Xiang, D. Gershlick, and C. Guardia for helpful discussions and critical review of the manuscript. This work was funded by the Intramural Program of the National Institute of Child Health and Human Development, NIH Grant ZIA HD001607.

1. Lasiecka ZM, Winckler B (2011) Mechanisms of polarized membrane trafficking in neurons – focusing in on endosomes. *Mol Cell Neurosci* 48(4):278–287.
2. Bonifacino JS (2014) Adaptor proteins involved in polarized sorting. *J Cell Biol* 204(1): 7–17.
3. Maeder CI, Shen K, Hoogenraad CC (2014) Axon and dendritic trafficking. *Curr Opin Neurobiol* 27:165–170.
4. Silverman MA, et al. (2001) Sorting and directed transport of membrane proteins during development of hippocampal neurons in culture. *Proc Natl Acad Sci USA* 98(13):7051–7057.
5. Sampo B, Kaech S, Kunz S, Banker G (2003) Two distinct mechanisms target membrane proteins to the axonal surface. *Neuron* 37(4):611–624.
6. Farías GG, et al. (2012) Signal-mediated, AP-1/clathrin-dependent sorting of transmembrane receptors to the somatodendritic domain of hippocampal neurons. *Neuron* 75(5):810–823.
7. Petersen JD, Kaech S, Banker G (2014) Selective microtubule-based transport of dendritic membrane proteins arises in concert with axon specification. *J Neurosci* 34(12):4135–4147.
8. Farías GG, Guardia CM, Britt DJ, Guo X, Bonifacino JS (2015) Sorting of dendritic and axonal vesicles at the pre-axonal exclusion zone. *Cell Reports* 13(6):1221–1232.
9. Simons M, et al. (1995) Intracellular routing of human amyloid protein precursor: Axonal delivery followed by transport to the dendrites. *J Neurosci Res* 41(1):121–128.
10. Burack MA, Silverman MA, Banker G (2000) The role of selective transport in neuronal protein sorting. *Neuron* 26(2):465–472.
11. Wisco D, et al. (2003) Uncovering multiple axonal targeting pathways in hippocampal neurons. *J Cell Biol* 162(7):1317–1328.
12. Garrido JJ, et al. (2003) A targeting motif involved in sodium channel clustering at the axonal initial segment. *Science* 300(5628):2091–2094.
13. Margeta MA, Wang GJ, Shen K (2009) Clathrin adaptor AP-1 complex excludes multiple postsynaptic receptors from axons in C. elegans. *Proc Natl Acad Sci USA* 106(5): 1632–1637.
14. Song AH, et al. (2009) A selective filter for cytoplasmic transport at the axon initial segment. *Cell* 136(6):1148–1160.
15. Al-Bassam S, Xu M, Wandless TJ, Arnold DB (2012) Differential trafficking of transport vesicles contributes to the localization of dendritic proteins. *Cell Reports* 2(1):89–100.
16. Choy RW, et al. (2014) Retromer mediates a discrete route of local membrane delivery to dendrites. *Neuron* 82(1):55–62.
17. Kuijpers M, et al. (2016) Dynein regulator NDEL1 controls polarized cargo transport at the axon initial segment. *Neuron* 89(3):461–471.
18. Dwyer ND, Adler CE, Crump JG, L'Etoile ND, Bargmann CI (2001) Polarized dendritic transport and the AP-1 mu1 clathrin adaptor UNC-101 localize odorant receptors to olfactory cilia. *Neuron* 31(2):277–287.
19. Mattera R, Farías GG, Mardones GA, Bonifacino JS (2014) Co-assembly of viral envelope glycoproteins regulates their polarized sorting in neurons. *PLoS Pathog* 10(5): e1004107.

20. Jain S, Farías GG, Bonifacino JS (2015) Polarized sorting of the copper transporter ATP7B in neurons mediated by recognition of a dileucine signal by AP-1. *Mol Biol Cell* 26(2):218–228.
21. Matsuda S, et al. (2008) Accumulation of AMPA receptors in autophagosomes in neuronal axons lacking adaptor protein AP-4. *Neuron* 57(5):730–745.
22. Matsuda S, Yuzaki M (2008) AP-4: Autophagy-four mislocalized proteins in axons. *Autophagy* 4(6):815–816.
23. Britt DJ, Farías GG, Guardia CM, Bonifacino JS (2016) Mechanisms of polarized organelle distribution in neurons. *Front Cell Neurosci* 10:88.
24. van Beuningen SF, Hoogenraad CC (2016) Neuronal polarity: Remodeling microtubule organization. *Curr Opin Neurobiol* 39:1–7.
25. Heidemann SR, Landers JM, Hamborg MA (1981) Polarity orientation of axonal microtubules. *J Cell Biol* 91(3 Pt 1):661–665.
26. Nakata T, Hirokawa N (2003) Microtubules provide directional cues for polarized axonal transport through interaction with kinesin motor head. *J Cell Biol* 162(6): 1045–1055.
27. Okada Y, Yamazaki H, Sekine-Aizawa Y, Hirokawa N (1995) The neuron-specific kinesin superfamily protein KIF1A is a unique monomeric motor for anterograde axonal transport of synaptic vesicle precursors. *Cell* 81(5):769–780.
28. Niwa S, Tanaka Y, Hirokawa N (2008) KIF1Bbeta- and KIF1A-mediated axonal transport of presynaptic regulator Rab3 occurs in a GTP-dependent manner through DENN/MADD. *Nat Cell Biol* 10(11):1269–1279.
29. Paschal BM, Vallee RB (1987) Retrograde transport by the microtubule-associated protein MAP 1C. *Nature* 330(6144):181–183.
30. Schnapp BJ, Reese TS (1989) Dynein is the motor for retrograde axonal transport of organelles. *Proc Natl Acad Sci USA* 86(5):1548–1552.
31. Waterman-Storer CM, et al. (1997) The interaction between cytoplasmic dynein and dynactin is required for fast axonal transport. *Proc Natl Acad Sci USA* 94(22): 12180–12185.
32. Baas PW, Deitch JS, Black MM, Banker GA (1988) Polarity orientation of microtubules in hippocampal neurons: Uniformity in the axon and nonuniformity in the dendrite. *Proc Natl Acad Sci USA* 85(21):8335–8339.
33. Setou M, Nakagawa T, Seog DH, Hirokawa N (2000) Kinesin superfamily motor protein KIF17 and mLin-10 in NMDA receptor-containing vesicle transport. *Science* 288(5472):1796–1802.
34. Saito N, et al. (1997) KIFC2 is a novel neuron-specific C-terminal type kinesin superfamily motor for dendritic transport of multivesicular body-like organelles. *Neuron* 18(3):425–438.
35. Kapitein LC, et al. (2010) Probing intracellular motor protein activity using an inducible cargo trafficking assay. *Biophys J* 99(7):2143–2152.
36. Wandinger-Ness A, Zerial M (2014) Rab proteins and the compartmentalization of the endosomal system. *Cold Spring Harb Perspect Biol* 6(11):a022616.
37. Angers CG, Merz AJ (2011) New links between vesicle coats and Rab-mediated vesicle targeting. *Semin Cell Dev Biol* 22(1):18–26.
38. Horgan CP, McCaffrey MW (2011) Rab GTPases and microtubule motors. *Biochem Soc Trans* 39(5):1202–1206.
39. Krämer H, Phistry M (1996) Mutations in the Drosophila hook gene inhibit endocytosis of the boss transmembrane ligand into multivesicular bodies. *J Cell Biol* 133(6): 1205–1215.
40. Xu L, et al. (2008) An FTS/Hook/p107(FHIP) complex interacts with and promotes endosomal clustering by the homotypic vacuolar protein sorting complex. *Mol Biol Cell* 19(12):5059–5071.
41. Gillingham AK, Sinka R, Torres IL, Lilley KS, Munro S (2014) Toward a comprehensive map of the effectors of rab GTPases. *Dev Cell* 31(3):358–373.
42. Bielska E, et al. (2014) Hook is an adapter that coordinates kinesin-3 and dynein cargo attachment on early endosomes. *J Cell Biol* 204(6):989–1007.
43. McKenney RJ, Huynh W, Tanenbaum ME, Bhabha G, Vale RD (2014) Activation of cytoplasmic dynein motility by dynactin-cargo adapter complexes. *Science* 345(6194): 337–341.
44. Zhang J, Qiu R, Arst HNJ, Jr, Peñalva MA, Xiang X (2014) HookA is a novel dynein-early endosome linker critical for cargo movement in vivo. *J Cell Biol* 204(6):1009–1026.
45. Xiang X, et al. (2015) Cytoplasmic dynein and early endosome transport. *Cell Mol Life Sci* 72(17):3267–3280.
46. Zhang X, Bennett V (1998) Restriction of 480/270-kD ankyrin G to axon proximal segments requires multiple ankyrin G-specific domains. *J Cell Biol* 142(6):1571–1581.
47. Cáceres A, Banker G, Steward O, Binder L, Payne M (1984) MAP2 is localized to the dendrites of hippocampal neurons which develop in culture. *Brain Res* 315(2):314–318.
48. Li G, Stahl PD (1993) Structure-function relationship of the small GTPase rab5. *J Biol Chem* 268(32):24475–24480.
49. Stenmark H, et al. (1994) Inhibition of rab5 GTPase activity stimulates membrane fusion in endocytosis. *EMBO J* 13(6):1287–1296.
50. Satoh D, et al. (2008) Spatial control of branching within dendritic arbors by dynein-dependent transport of Rab5-endosomes. *Nat Cell Biol* 10(10):1164–1171.
51. Zhang H, et al. (2014) Endocytic pathways downregulate the L1-type cell adhesion molecule neuroglian to promote dendrite pruning in Drosophila. *Dev Cell* 30(4): 463–478.
52. Bucci C, et al. (1995) Co-operative regulation of endocytosis by three Rab5 isoforms. *FEBS Lett* 366(1):65–71.
53. de Hoop MJ, et al. (1994) The involvement of the small GTP-binding protein Rab5a in neuronal endocytosis. *Neuron* 13(1):11–22.
54. Brown TC, Tran IC, Backos DS, Esteban JA (2005) NMDA receptor-dependent activation of the small GTPase Rab5 drives the removal of synaptic AMPA receptors during hippocampal LTD. *Neuron* 45(1):81–94.
55. Deinhardt K, et al. (2006) Rab5 and Rab7 control endocytic sorting along the axonal retrograde transport pathway. *Neuron* 52(2):293–305.
56. Zheng Y, et al. (2008) Dynein is required for polarized dendritic transport and uniform microtubule orientation in axons. *Nat Cell Biol* 10(10):1172–1180.
57. Kapitein LC, et al. (2010) Mixed microtubules steer dynein-driven cargo transport into dendrites. *Curr Biol* 20(4):290–299.
58. King SJ, Brown CL, Maier KC, Quintyne NJ, Schroer TA (2003) Analysis of the dynein-dynactin interaction in vitro and in vivo. *Mol Biol Cell* 14(12):5089–5097.
59. Burkhardt JK, Echeverri CJ, Nilsson T, Vallee RB (1997) Overexpression of the dynamitin (p50) subunit of the dynactin complex disrupts dynein-dependent maintenance of membrane organelle distribution. *J Cell Biol* 139(2):469–484.
60. Quintyne NJ, et al. (1999) Dynactin is required for microtubule anchoring at centrosomes. *J Cell Biol* 147(2):321–334.
61. Nielsen E, Severin F, Backer JM, Hyman AA, Zerial M (1999) Rab5 regulates motility of early endosomes on microtubules. *Nat Cell Biol* 1(6):376–382.
62. Ohya T, et al. (2009) Reconstitution of Rab- and SNARE-dependent membrane fusion by synthetic endosomes. *Nature* 459(7250):1091–1097.
63. Miaczynska M, et al. (2004) APPL proteins link Rab5 to nuclear signal transduction via an endosomal compartment. *Cell* 116(3):445–456.
64. Walenta JH, Didier AJ, Liu X, Krämer H (2001) The Golgi-associated hook3 protein is a member of a novel family of microtubule-binding proteins. *J Cell Biol* 152(5):923–934.
65. Yao X, Wang X, Xiang X (2014) FHIP and FTS proteins are critical for dynein-mediated transport of early endosomes in Aspergillus. *Mol Biol Cell* 25(14):2181–2189.
66. Szebenyi G, Hall B, Yu R, Hashim AI, Krämer H (2007) Hook2 localizes to the centrosome, binds directly to centriolin/CEP110 and contributes to centrosomal function. *Traffic* 8(1):32–46.
67. Maldonado-Báez L, Cole NB, Krämer H, Donaldson JG (2013) Microtubule-dependent endosomal sorting of clathrin-independent cargo by Hook1. *J Cell Biol* 201(2): 233–247.
68. Stenmark H, Vitale G, Ullrich O, Zerial M (1995) Rabaptin-5 is a direct effector of the small GTPase Rab5 in endocytic membrane fusion. *Cell* 83(3):423–432.
69. Delprato A, Merithew E, Lambright DG (2004) Structure, exchange determinants, and family-wide rab specificity of the tandem helical bundle and Vps9 domains of Rabex-5. *Cell* 118(5):607–617.
70. Mattera R, Bonifacino JS (2008) Ubiquitin binding and conjugation regulate the recruitment of Rabex-5 to early endosomes. *EMBO J* 27(19):2484–2494.
71. Herrmann L, et al. (2015) Hook proteins: Association with Alzheimer pathology and regulatory role of hook3 in amyloid beta generation. *PLoS One* 10(3):e0119423.
72. Futter CE, Connolly CN, Cutler DF, Hopkins CR (1995) Newly synthesized transferrin receptors can be detected in the endosome before they appear on the cell surface. *J Biol Chem* 270(18):10999–11003.
73. Orzech E, Cohen S, Weiss A, Aroeti B (2000) Interactions between the exocytic and endocytic pathways in polarized Madin-Darby canine kidney cells. *J Biol Chem* 275(20):15207–15219.
74. Watanabe K, et al. (2012) Networks of polarized actin filaments in the axon initial segment provide a mechanism for sorting axonal and dendritic proteins. *Cell Reports* 2(6):1546–1553.
75. Delcroix JD, et al. (2003) NGF signaling in sensory neurons: Evidence that early endosomes carry NGF retrograde signals. *Neuron* 39(1):69–84.
76. Deinhardt K, Reversi A, Berninghausen O, Hopkins CR, Schiavo G (2007) Neurotrophins Redirect p75NTR from a clathrin-independent to a clathrin-dependent endocytic pathway coupled to axonal transport. *Traffic* 8(12):1736–1749.
77. Salinas S, et al. (2009) CAR-associated vesicular transport of an adenovirus in motor neuron axons. *PLoS Pathog* 5(5):e1000442.
78. Cantalupo G, Alifano P, Roberti V, Bruni CB, Bucci C (2001) Rab-interacting lysosomal protein (RILP): The Rab7 effector required for transport to lysosomes. *EMBO J* 20(4): 683–693.
79. Jordens I, et al. (2001) The Rab7 effector protein RILP controls lysosomal transport by inducing the recruitment of dynein-dynactin motors. *Curr Biol* 11(21):1680–1685.
80. Johansson M, Lehto M, Tanhuanpää K, Cover TL, Olkkonen VM (2005) The oxysterol-binding protein homologue ORP1L interacts with Rab7 and alters functional properties of late endocytic compartments. *Mol Biol Cell* 16(12):5480–5492.
81. Yang Y, et al. (2001) The gene encoding alsin, a protein with three guanine-nucleotide exchange factor domains, is mutated in a form of recessive amyotrophic lateral sclerosis. *Nat Genet* 29(2):160–165.
82. Hafezparast M, et al. (2003) Mutations in dynein link motor neuron degeneration to defects in retrograde transport. *Science* 300(5620):808–812.
83. Münch C, et al. (2004) Point mutations of the p150 subunit of dynactin (DCTN1) gene in ALS. *Neurology* 63(4):724–726.
84. Vitale G, et al. (1998) Distinct Rab-binding domains mediate the interaction of Rabaptin-5 with GTP-bound Rab4 and Rab5. *EMBO J* 17(7):1941–1951.
85. Mattera R, Tsai YC, Weissman AM, Bonifacino JS (2006) The Rab5 guanine nucleotide exchange factor Rabex-5 binds ubiquitin (Ub) and functions as a Ub ligase through an atypical Ub-interacting motif and a zinc finger domain. *J Biol Chem* 281(10): 6874–6883.
86. Mori Y, Matsui T, Fukuda M (2013) Rabex-5 protein regulates dendritic localization of small GTPase Rab17 and neurite morphogenesis in hippocampal neurons. *J Biol Chem* 288(14):9835–9847.
87. Kaech S, Banker G (2006) Culturing hippocampal neurons. *Nat Protoc* 1(5):2406–2415.
88. Mattera R, Arighi CN, Lodge R, Zerial M, Bonifacino JS (2003) Divalent interaction of the GGAs with the Rabaptin-5-Rabex-5 complex. *EMBO J* 22(1):78–88.